Ultrastructural and Biochemical Localization of N-RAP at the Interface between Myofibrils and Intercalated Disks in the Mouse Heart

Jian Q. Zhang,[‡] Brian Elzey,[§] Greg Williams,[§] Shajia Lu,[‡] Douglas J. Law,[§] and Robert Horowits*[,‡]

Laboratory of Muscle Biology, National Institute of Arthritis and Musculoskeletal and Skin Diseases, National Institutes of Health, Bethesda, Maryland 20892, and Division of Cell Biology and Biophysics, University of Missouri, Kansas City, Missouri 64110

Received April 12, 2001; Revised Manuscript Received September 18, 2001

ABSTRACT: N-RAP is a recently discovered muscle-specific protein found at cardiac intercalated disks. Double immunogold labeling of mouse cardiac muscle reveals that vinculin is located immediately adjacent to the fascia adherens region of the intercalated disk membrane, while N-RAP extends ∼100 nm further toward the interior of the cell. We partially purified cardiac intercalated disks using low- and high-salt extractions followed by density gradient centrifugation. Immunoblots show that this preparation is highly enriched in desmin and junctional proteins, including N-RAP, talin, vinculin, β1-integrin, N-cadherin, and connexin 43. Electron microscopy and immunolabeling demonstrate that N-RAP and vinculin are associated with the large fragments of intercalated disks that are present in this preparation, which also contains numerous membrane vesicles. Detergent treatment of the partially purified intercalated disks removed the membrane vesicles and extracted vinculin and β1-integrin. Further separation on a sucrose gradient removed residual actin and myosin and yielded a fraction morphologically similar to fasciae adherentes that was highly enriched in N-RAP, N-cadherin, connexin 43, talin, desmin, and α-actinin. The finding that N-RAP copurifies with detergent-extracted intercalated disk fragments even though β-integrin and vinculin have been completely removed suggests that N-RAP association with the adherens junction region is mediated by the cadherin system. Consistent with this hypothesis, we found that recombinant N-RAP fragments bind α-actinin in a gel overlay assay. In addition, immunofluorescence shows that N-RAP remains bound at the ends of isolated, detergent-treated cardiac myofibrils. These results demonstrate that N-RAP remains tightly bound to myofibrils and fasciae adherentes during biochemical purification and may be a key constituent in the mechanical link between these two structures.

N-RAP is a recently discovered protein found in skeletal and cardiac muscles (*1*). Analysis of the N-RAP cDNA identified two regions with homology to previously characterized domains. The C-terminal half of mouse N-RAP contains repeating modules homologous to those found in nebulin (*1*), a giant actin binding protein thought to regulate actin filament length in skeletal muscle sarcomeres (*2*−*4*). N-RAP contains 17 of these weakly repeating 35 residue modules, that are in turn organized into ∼2.5 superrepeat regions of seven modules each (*1*). N-RAP also contains a consensus sequence for a LIM domain at its N-terminal end (*1*). LIM domains are cysteine-rich regions that bind two zinc ions, forming two adjacent zinc-finger-like structures. In general, LIM domains are thought to mediate protein−protein interactions (*5*, *6*). In vitro binding studies on recombinant N-RAP fragments demonstrated specific, high-affinity interactions between the N-RAP LIM domain and talin, while the N-RAP superrepeats bound both actin and vinculin (*7*).

In adult tissues, N-RAP is concentrated at the myotendinous junctions of skeletal muscle and at the intercalated disks of cardiac muscle (*1*). Using immunoelectron microscopy, we recently showed that N-RAP is specifically associated with the terminal bundles of actin filaments at the myotendinous junctions (*8*). In addition, N-RAP was found concentrated at the cell periphery along with the earliest detectable myofibril precursors in spreading cultures of embryonic chick cardiomyocytes (*9*).

Taken together, previous observations suggested that N-RAP may function as a mechanical link between myofibrils and the cell membrane that persists from the initial genesis of the myofibrils to the adult muscle (*1*, *7*, *9*). In the present study, we tested this hypothesis by studying the linkage between myofibril ends and the membrane in adult mouse cardiac muscle. In cardiomyocytes, the myofibrils terminate at the intercalated disk, which contains regions of tight mechanical attachment (fasciae adherentes and desmosomes) and electrical coupling (gap junctions) between adjacent cells (*10*, *11*). The fasciae adherentes contain the transmembrane protein N-cadherin, which interacts with identical molecules from neighboring cells to form a tight mechanical intercellular link (*12*−*15*). At the intracellular face of the fasciae adherentes, the terminal sarcomeres of the myofibrils are coupled to the membane by a series of proteins that interact to form a mechanically strong link with the terminal actin filaments; proteins thought to be involved in this link include α-actinin and vinculin (*16*), talin (*17*), β1D-integrin (*18*), and the catenins (*19*). The intracellular

* Corresponding author: Building 6, Room 408, MSC 2751, National Institutes of Health, Bethesda, MD 20892-2751. Telephone 301-435-8371; fax 301-402-0009; e-mail horowits@helix.nih.gov.

[‡] National Institute of Arthritis and Musculoskeletal and Skin Diseases, NIH.

[§] University of Missouri.

10.1021/bi0107445 CCC: $20.00
Published on Web 11/10/2001

myofibril to membrane link and the intercellular cadherin-mediated link are both essential for appropriate transmission of forces in the whole heart.

Here we address the ultrastructural localization and biochemical association of N-RAP at the interface between myofibrils and membranes in adult mouse hearts. The results show that N-RAP is located near the fascia adherens membrane and remains tightly bound to myofibril termini during biochemical purification. Furthermore, N-RAP copurifies with several other intercalated disk components after tissue extraction and density gradient centrifugation. These results are consistent with N-RAP's putative role as a tension-bearing mechanical link between myofibrils and intercalated disks.

MATERIALS AND METHODS

Antibodies. Polyclonal antibody against N-RAP has been previously described (*1*). Polyclonal rabbit antibodies against connexin 43 and myosin, as well as monoclonal antibodies against desmin (clone DE-U-10), talin (clone 8D4), vinculin (clones VIN-11-5 and hVIN-1), and sarcomeric α-actinin (clone EA-53) were obtained from Sigma Chemical Co. (St. Louis, MO). Monoclonal antibodies against actin (clone C4), N-cadherin (RDI-NCADHERabm), and β1-integrin (clone DF5) were obtained from Boehringer Mannheim Corp. (Indianapolis, IN), Research Diagnostics, Inc. (Flanders, NJ), and Chemicon International, Inc. (Temecula, CA), respectively.

Myofibril Preparation and Immunofluorescence. Myofibrils were prepared with minor modifications of previously described methods (*20*). All steps were performed at 4 °C, and a 1:100 dilution of protease inhibitor cocktail (Sigma Chemical Co., St. Louis, MO) was included in all solutions. In brief, hearts were dissected from adult mice, cut in half, and chemically skinned in a rigor solution [75 mM KCl, 10 mM tris(hydroxymethyl)aminomethane (Tris), 2 mM $MgCl_2$, and 2 mM ethylene glycol bis(β-aminoethyl ether)-*N*,*N*,*N*′,*N*′-tetraacetic acid (EGTA), pH 6.8] containing 0.1% Triton-X-100 during a 2 h incubation at 4 °C. The tissue was homogenized in ~10 volumes of the same buffer with an Omni 2000 homogenizer (Omni International, Inc., Gainesville, VA), and then centrifuged at 800*g* for 10 min at 4 °C. The pelleted myofibrils were resuspended in rigor solution and passed through two layers of cheesecloth. They were then washed three times by centrifugation at 800*g* for 10 min, followed by resuspension in fresh rigor solution, and were finally resuspended in rigor solution and diluted 1:1 with glycerol for storage at −20 °C.

Myofibrils were stained for N-RAP in flow chambers as previously described (*8*). In brief, they were incubated for 30 min in blocking solution [5% goat serum in phosphate-buffered saline (PBS)], followed by a 1 h incubation with anti-N-RAP antibody diluted 1:1000 in blocking solution, and then a 1 h incubation with fluorescein-linked antibody from donkey against rabbit immunoglobulins (Amersham Corp., Arlington Heights, IL) diluted 1:20 in blocking solution. After each incubation, unbound antibody was washed out with blocking solution. The stained myofibrils were mounted in a 1:1 mixture of PBS and Vectashield mounting medium (Vector Laboratories, Burlingame, CA). They were viewed and photographed by use of a Zeiss Axiovert 135 microscope equipped for incident-light fluorescence and phase-contrast microscopy (Carl Zeiss, Thornwood, NY). Digital micrographs were captured with a Hamamatsu CCD camera and controller interfaced with a Power Macintosh computer. The objective was a 100× plan-neofluar oil immersion objective having a numerical aperture of 1.30.

Intercalated Disk Preparations. Mouse hearts were fractionated by a protocol modified from that of Colaco and Evans (*21*). All steps were performed at 4 °C, and a 1:100 dilution of protease inhibitor cocktail (Sigma) was included in all solutions. Aliquots were taken at each step for analysis by gel electrophoresis and immunoblot by standard techniques (*22*).

Hearts were dissected 6−8 weeks after birth from 30−100 C57black/6 mice. The pooled tissue, weighing between 3 and 10 g, was rinsed in Tris buffer (10 mM Tris-HCl, pH 7.0). Each 1.0−1.5 g of tissue was homogenized in 30 mL of Tris buffer in an Omni 2000 homogenizer, followed by 40−50 strokes in a Dounce homogenizer. The homogenate was filtered through 16 layers of cheesecloth and then centrifuged for 20 min at 10000*g*. Each pellet was resuspended in 30 mL of KCl extraction buffer (0.6 M KCl, 8% sucrose, and 10 mM Tris, pH 7.0). The resuspended pellets were pooled and stirred overnight and then centrifuged for 20 min at 10000*g*. The pellets were pooled and resuspended in 12−38 mL of Tris buffer containing 25% sucrose. The resuspended material was loaded onto a sucrose gradient composed of four steps containing 37%, 45%, 50%, and 54% sucrose in Tris buffer. The sucrose gradients were centrifuged at 98000*g* for 2 h, and the material at each interface was collected; the fractions collected at the 25%/37%, 37%/45%, 45%/50%, and 50%/54% sucrose interfaces were labeled T1, F1, F2, and F3, respectively.

A portion of the F3 fraction was mixed 1:1 with a detergent extraction buffer (10% *N*-lauryl sarcosinate and 0.45 M Tris-HCl, pH 7.8) and incubated with occasional mixing for 30 min. After extraction, the mixture was centrifuged at 98000*g* for 20 min. The pelleted detergent-insoluble material was resuspended in 2−12 mL of Tris buffer containing 25% sucrose and 0.5% Triton X-100. The resuspended material was loaded onto a sucrose gradient composed of four steps containing 37%, 45%, 54%, and 72% sucrose in Tris buffer containing 0.1% Triton X-100. The sucrose gradients were centrifuged at 98000*g* for 2 h, and the material at each interface was collected; the fractions collected at the top three interfaces were pooled and labeled T2, and the material at the 54%/72% sucrose interface was labeled F3′.

Electron Microscopy. The hearts of freshly sacrificed adult mice (strain C57BL10/SnJ) were dissected out, briefly placed in PBS at 37 °C where continued beating cleared blood from the heart chambers, and then fixed by immersion in 2% paraformaldehyde in PBS for 4−6 h at 4 °C. Hearts were rinsed in PBS, then papillary muscles were removed and cut into blocks of <1 mm^3. Samples were infused overnight at 4 °C with a mixture of 2.1 M sucrose and 10% poly(vinylpyrrolidone) (PVP) and then mounted on specimen supports and frozen in liquid nitrogen prior to cryosectioning (*23*). Sections approximately 1.5 μm thick were examined by phase-contrast light microscopy; longitudinally oriented samples were sectioned at 80−100 nm thickness for electron microscopy. Sections were incubated for 90 min in a mixture

of rabbit anti-N-RAP (*1*) and mouse anti-vinculin (clone hVIN-1, Sigma, St. Louis, MO) with both antibodies at a final dilution of 1:50. Bound antibodies were detected with a mixture of species-specific secondary antibodies conjugated to 6 nm (goat anti-mouse IgG) or 12 nm (goat anti-rabbit IgG) colloidal gold, each at a 1:50 dilution. The secondary antibodies (Jackson Immunoresearch, West Grove, PA) were each adsorbed against serum proteins from the nontarget species, to minimize cross-reactivity with the nontarget primary antibody. Standard blocking and washing steps were included in the labeling procedure, as described previously (*8*). Sections were viewed and photographed by use of a Jeol 1200EX transmission electron microscope, at an accelerating voltage of 100 kV.

Selected fractions recovered from sucrose gradients were diluted 5-fold with Tris buffer and pelleted by centrifugation at 16000*g* for 15 min. For standard transmission electron microscopy, the pellets were fixed overnight in cacodylate buffer (0.15 M sodium cacodylate, pH 7.2) containing 2% glutaraldehyde. The pellets were washed with cacodylate buffer, and postfixed for 1 h at 4 °C with 1% OsO_4 in 100 mM KH_2PO_4 and 10 mM $MgCl_2$, pH 6.0. Samples were rinsed, dehydrated, embedded, sectioned, and stained according to published protocols (*24*). Pellets used for immunolabeling were fixed for 2 h in PBS containing 2% paraformaldehyde. These pellets were washed in PBS, then cryoprotected with the above sucrose/PVP mixture, mounted on specimen supports, and frozen in liquid nitrogen. Cryosections were obtained, immunolabeled, viewed, and photographed as above.

Recombinant N-RAP Expression. Recombinant mouse N-RAP fragments containing an N-terminal histidine tag were expressed in *Escherichia coli* and purified as previously described (*1*, *7*). These fragments include N-RAP−SR, which contains more than 10 complete modules from the nebulin-related N-RAP superrepeats, and N-RAP−IB, which includes most of the region between the superrepeats and the N-RAP LIM domain. Recombinant chloramphenicol acetyltransferase with an N-terminal histidine tag (HIS−CAT-1) was similarly expressed and purified by use of the pPROEX-HT-Cat plasmid vector (Life Technologies, Inc., Gaithersburg, MD).

In addition, we cloned and expressed the N-RAP LIM domain as a fusion protein containing an N-terminal histidine tag. The cDNA coding for the LIM domain was amplified by polymerase chain reaction (PCR) from a previously characterized mouse N-RAP clone with forward (5′-CACCATGAATGTGCAGGCCTGCTCT-3′) and reverse (5′-CTAGTGGGCGTGACAGTACGG-3′) primers designed to amplify nucleotides 1523−1693 of the N-RAP sequence. The PCR reaction was performed with the ThermalAce DNA polymerase kit (Invitrogen, Carlsbad, CA) in a 50 μL volume containing 0.3 ng of the template plasmid DNA, 0.5 μM each primer, 2 units of the ThermalAce DNA polymerase, 200 μM each dNTP, 60 mM Tris-HCl (pH 9.25), 1.5 mM $MgSO_4$, 30 mM NaCl, 0.05 μg of bovine serum albumin, and 0.01% Triton X-100. Thermal cycling was accomplished by use of a PTC-200 DNA engine thermal cycler (MJ Research, Inc., Waltham, MA) programmed as follows: 1 cycle at 95 °C for 3 min; 30 cycles at 95 °C for 30 s and then 68 °C for 5 min; and 1 cycle at 74 °C for 7 min. The gel-purified PCR product was cloned and expressed in the Echo cloning and expression system (Invitrogen, Carlsbad, CA) according to the manufacturer's protocol. In brief, the PCR product was cloned into the pUniD/V5-His-TOPO plasmid donor vector with the vector-associated topoisomerase and then transferred by recombination into the pRSET-E plasmid acceptor vector with Cre recombinase. Positive clones were identified by restriction enzyme analysis with *Xba*I and *Eco*RV, and the integrity of the recombination sites and the insert were confirmed by sequencing the plasmid.

The N-RAP-LIM expression plasmid was transformed into BL21(DE3)pLysS host *E. coli* cells (Invitrogen, Inc., Carlsbad, CA). Bacterial cells harboring the expression plasmids were cultured in 1−2 L of LB medium with 50 μg/mL kanamycin and 34 μg/mL chloramphenicol at 37 °C. Three hours later the expression of N-RAP-LIM was induced by the addition of isopropyl thio-β-D-galactoside (IPTG) to a final concentration of 0.75 mM. Cells were pelleted 4 h after induction by centrifugation at 4000*g* for 15 min at 4 °C and then resuspended in $^1/_{10}$ culture volume of a lysis buffer of 100 mM NaH_2PO_4, 10 mM Tris-HCl (pH 8.0), 8 M urea, 1 mM phenylmethanesulfonyl fluoride (PMSF), and 1:100 protease inhibitor cocktail for use in the purification of poly(histidine)-tagged proteins (Sigma Chemical Co., St. Louis, MO). The cells were lysed with three cycles of freezing on dry ice and thawing at 50 °C, followed by sonication at high setting for 2 min in a Branson Sonifier 250 sonicator (Branson Ultrasonics Corp., Danbury, CT). The homogenates were centrifuged at 10000*g* for 20 min at 4 °C. The expressed histidine-tagged LIM proteins in the supernatants were purified with Ni−NTA resin (Qiagen, Inc.). Recombinant chloramphenicol acetyltransferase with an N-terminal histidine tag (HIS−CAT-2) was similarly expressed and purified by use of the pRSET-E/Uni-CAT control vector (Invitrogen, Inc., Carlsbad, CA).

α-*Actinin Binding to Blotted Proteins*. Gel overlay binding assays were performed as previously described (*1*). Recombinant proteins purified as described above, along with α-actinin purified from rabbit skeletal muscle (Cytoskeleton, Inc., Denver, CO) and rainbow molecular weight standards (Amersham Pharmacia Biotech, Piscataway, NJ) were electrophoresed under denaturing conditions and blotted to polyvinylidene difluoride (PVDF) membranes. Membranes were washed for 3 × 10 min with a wash buffer containing 0.2% Tween-20 and PBS, pH 7.4. They were then incubated at 4 °C overnight in a blocking buffer containing 10% nonfat dry milk in wash buffer, followed by 5 × 5 min in wash buffer. The membranes were incubated overnight at 4 °C with 10 μg/mL (0.1 μM) α-actinin (Cytoskeleton, Inc., Denver, CO) in binding buffer [100 mM KCl, 50 mM Tris-HCl (pH 7.4), 1 mM EGTA, 2 mM $MgCl_2$, 2 mM ATP, 0.3 mM dithiothreitol (DTT), and 0.2% Tween-20]. Following the incubation, membranes were washed for 5 × 5 min with binding buffer. Bound α-actinin was detected by primary monoclonal antibody against sarcomeric α-actinin (Sigma, St. Louis, MO) followed by horseradish peroxidase conjugated anti-mouse Ig (Amersham Corp., Arlington Heights, IL); the primary and secondary antibodies were diluted 1:1000 and 1:5000, respectively, in binding buffer, and unbound antibodies were removed by subsequent washing in binding buffer. The ECL Western blot system was used for detection of bound antibody (Amersham Pharmacia Biotech, Inc.).

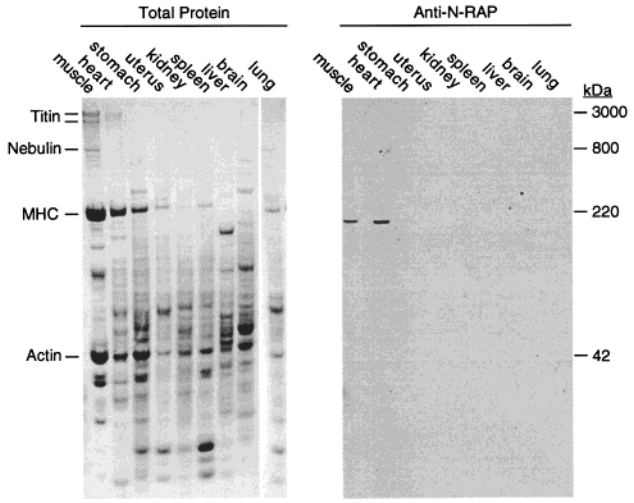

FIGURE 1: Immunoblot analysis of N-RAP expression in adult mouse tissues. Lanes were loaded with equivalent amounts of protein from whole homogenates of the indicated tissues. The left-hand panel shows the staining for total protein with Coomassie blue, and the right-hand panel shows the immunoblot probed with anti-N-RAP antiserum. N-RAP is only expressed in skeletal muscle and heart and is not detected in nonmuscle tissues or in organs enriched in smooth muscle, such as the stomach and uterus. MHC, myosin heavy chain.

RESULTS

Tissue Specificity of N-RAP Expression. Immunoblot analysis of N-RAP expression in whole homogenates of adult mouse tissues shows that it is expressed in skeletal muscle and heart but is not detected in a wide variety of other tissues (Figure 1). In addition to the nonmuscle tissues (kidney, spleen, liver, brain, and lung), N-RAP was not detected in either stomach or uterus, tissues rich in smooth muscle cells. These results demonstrate that N-RAP is only expressed in the striated muscles.

Ultrastructural Localization of N-RAP in Adult Hearts. Frozen sections of adult mouse hearts were double-labeled for vinculin and N-RAP. Figure 2A shows a region containing the cardiac intercalated disk. The terminal sarcomeres of the myofibrils are clearly visible, along with the adherens junctions to which they are attached. Interestingly, the 12 nm diameter gold particles that mark the N-RAP labeling are concentrated in the fascia adherens region but are typically not observed within the sarcomeres themselves. At higher magnifications, the 6 nm gold particles that mark the vinculin labeling are clearly visible, marking the membrane region of the fascia adherens (Figure 2B). The N-RAP labeling does not colocalize with vinculin at the membrane but instead lies within the terminal cell process, overlaying the terminal actin filaments that are thought to link the myofibrils to the membrane. Omission of primary antibody or substitution of preimmune serum results in no significant deposition of gold particles (Figure 2C).

N-RAP in Isolated Myofibrils. Many isolated, detergent-treated cardiac myofibrils have phase-dense remnants of intercalated disks at their ends (Figure 3, arrowheads). These remnants are stained by anti-N-RAP antibody but not by preimmune serum (panels A and B, respectively). The results show that N-RAP remains tightly bound to the ends of cardiac myofibrils during biochemical purification and extraction with detergent.

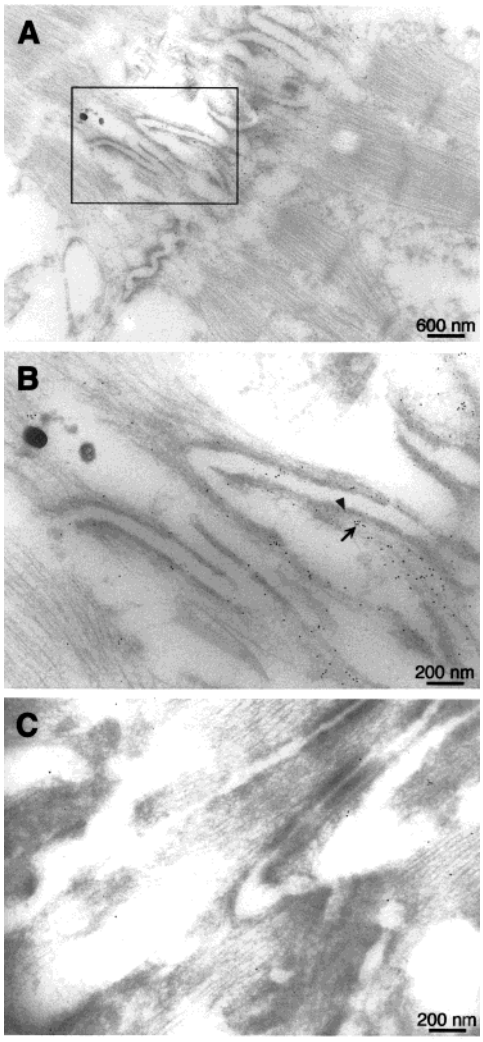

FIGURE 2: Immunoelectron microscopy of frozen adult mouse heart. N-RAP and vinculin were detected with secondary antibodies conjugated with 12 and 6 nm colloidal gold, respectively. The top panel (A) shows an overview of the intercalated disk region; the center panel (B) shows the boxed region at higher magnification. Vinculin labeling marks the intercalated disk membrane (arrowhead), while N-RAP labeling is found near, but not at, the membrane (arrow). The bottom panel (C) shows a control sample exposed to preimmune serum and both secondary antibodies.

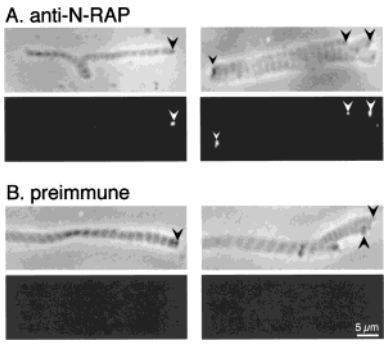

FIGURE 3: Each pair of micrographs shows isolated cardiac myofibrils illuminated for phase contrast (top panels) and immunofluorescence (bottom panels). The phase-dense remnants of intercalated disks (arrowheads) are specifically labeled by N-RAP antiserum (A) but remain unstained by preimmune serum (B).

N-RAP in Isolated Intercalated Disks. We fractionated mouse hearts using a protocol modified from Colaco and Evans (*21*) (Figure 4). The initial steps consisted of sequential

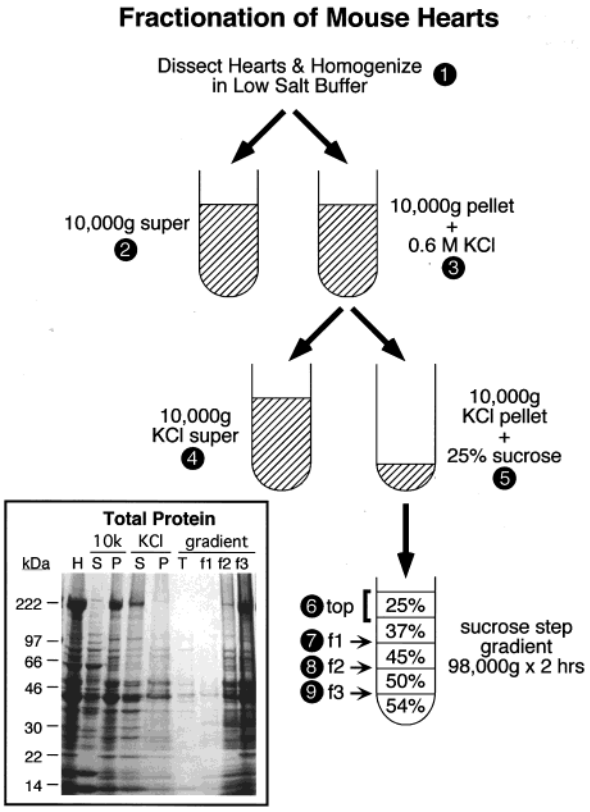

FIGURE 4: Schematic diagram illustrating the protocol for fractionation of mouse hearts. The inset shows the proteins from each step of the procedure separated on a denaturing gel. Numbers at each step in the schematic refer to the loading order on the gel, from left to right. To compare the relative amounts of protein recovered in each fraction, a fixed percentage of the total fraction volume was loaded for each sample; the amount loaded represents a 10-fold greater percentage of the recovered material for the fractions collected from the sucrose gradient than for the preceding fractions. Note that the bulk of the actin (42 kDa) and myosin heavy chain (220 kDa) has been extracted from the KCl pellet fraction, which was loaded on the gradient.

low-salt and high-salt extractions, which removed most of the contractile proteins such as actin and myosin (Figure 4, inset). The remaining insoluble material was fractionated on a sucrose step gradient (Figure 4). Immunoblot analysis of the fractions reveals that all of the N-RAP is recovered in F3, the material collected from the 50%/54% sucrose interface (Figure 5). Visual inspection of the immunoblots shows that over 80% of each of the integral membrane proteins N-cadherin, β1-integrin, and connexin 43 were also recovered in this fraction (Figure 5), indicating that this fraction was enriched for intercalated disks. In addition, 50−75% of the cytoskeletal adapter proteins talin and vinculin were found in F3, as well as virtually all of the desmin (Figure 5), the major intermediate filament protein found in striated muscles. Densitometry of the Coomassie-stained gels shows that approximately 10% of the total homogenate protein was recovered in the F3 fraction. Therefore, the integral membrane proteins and cytoskeletal adapter proteins, including N-RAP, were enriched 5−10-fold in this fraction. In contrast, more than 80% of each of the major myofibrillar proteins probed, such as myosin and α-actinin (Figure 5), as well as actin (data not shown), were removed by the initial low- and high-salt extractions. Nevertheless, most of what remained of these in the KCl pellet were also recovered from the sucrose gradient in the F3 fraction (Figure 5).

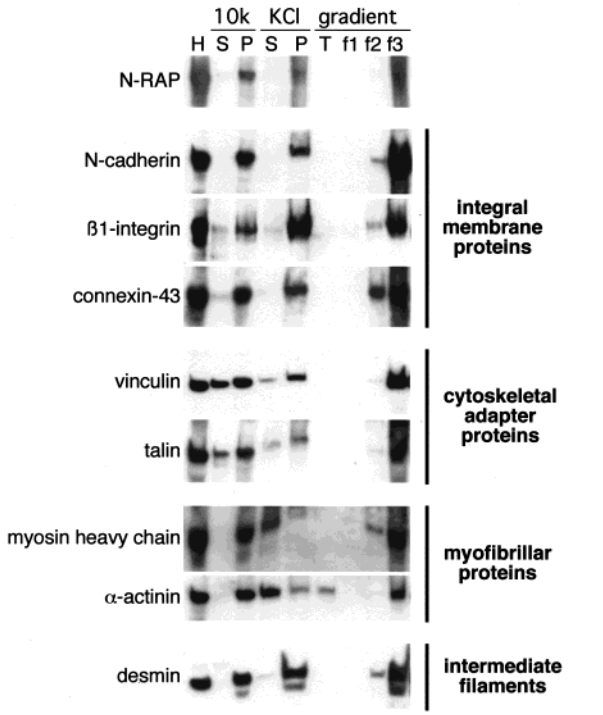

FIGURE 5: Immunoblot analysis of the fractions collected during preparation of crude intercalated disks. Labeling and loading is as shown in Figure 4. Note that virtually all of the N-RAP is recovered in the F3 fraction.

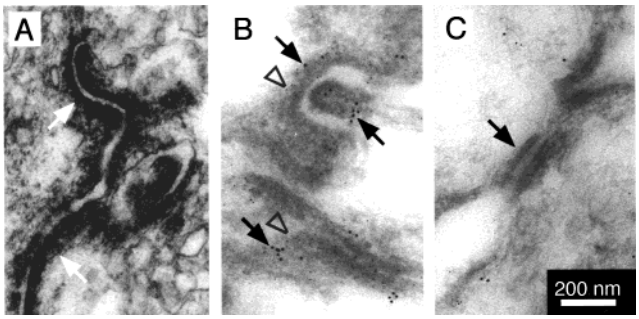

FIGURE 6: Ultrastructural analysis of F3, the crude intercalated disk preparation recovered from the sucrose gradient. (A) Micrographs of embedded specimens reveal the presence of structures resembling fragments of intercalated disks (arrows), along with numerous membrane vesicles. (B, C) Frozen specimens double-labeled with antibodies against N-RAP and vinculin, which were detected with secondary antibodies conjugated with 12 and 6 nm colloidal gold, respectively. Panel B shows a fascia adherens region of an intercalated disk, with significant labeling for both N-RAP (arrows) and vinculin (open arrowheads). Panel C shows a desmosome (arrow), with no significant labeling for either N-RAP or vinculin.

Transmission electron microscopy of the F3 fraction reveals the presence of structures resembling fragments of intercalated disks, along with numerous membrane vesicles (Figure 6A). When frozen sections of this fraction were double-labeled with antibodies against vinculin and N-RAP, we found that both proteins were localized at structures resembling fragments of adherens junctions (Figure 6B). Vinculin was generally at the membrane of these structures (Figure 6B, open arrowheads), while N-RAP was colocalized with the adjacent filamentous material (Figure 6B, arrows). In contrast, desmosomal junctions present in this fraction were unlabeled by either N-RAP or vinculin antibodies (Figure 6C).

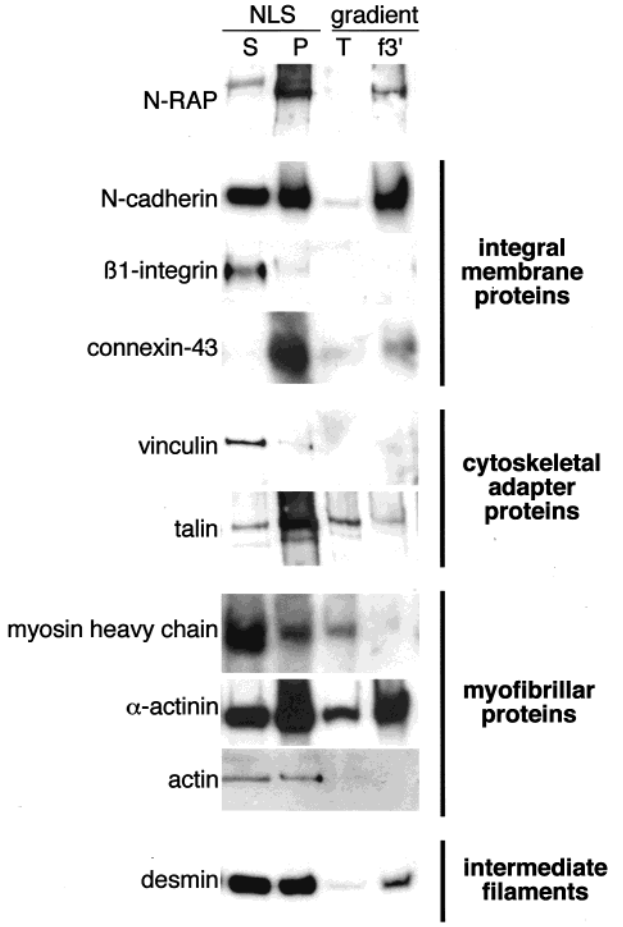

FIGURE 7: Immunoblot analysis of the fractions collected after detergent extraction of the crude intercalated disk fraction (F3) with *N*-lauryl sarcosinate (NLS), followed by sucrose gradient centrifugation of the insoluble pellet. S and P are lanes loaded with the supernatant and pellet fractions, respectively, following NLS extraction. T is material pooled from the 25%/37%, 37%/45%, and 45%/54% sucrose interfaces. F3′ is the material collected from the 54%/72% sucrose interface. Note that most of the N-RAP is recovered in the F3′ fraction.

We attempted to further purify the intercalated disk fragments by detergent extraction with *N*-lauryl sarcosinate followed by separation on a sucrose gradient. The immunoblot analyses indicate that most of the β1-integrin, vinculin, and myosin are removed by the detergent (Figure 7). In contrast, most of the N-RAP, connexin 43, talin, and α-actinin present in the crude intercalated disk fraction (F3) resist extraction with *N*-lauryl sarcosinate, along with half of the remaining N-cadherin, actin, and desmin (Figure 7). Subsequent sucrose gradient centrifugation resulted in recovery of most of the detergent-insoluble components at the 54%/72% sucrose interface (F3′); however, this step effectively removed the trace amounts of myosin and actin that were present (Figure 7), with myosin found in the fraction consisting of the pooled interfaces that were less dense than F3′ (Figure 7), and actin found in the small pellet recovered after centrifugation (data not shown). Figure 8A illustrates the total proteins recovered from the supernatant and pellet after detergent extraction, as well as the proteins recovered from the subsequent sucrose gradient centrifugation step. The fractions recovered after detergent extraction are extremely insoluble, and much of the final F3′ fraction does not enter the gel; nevertheless, most of the major protein

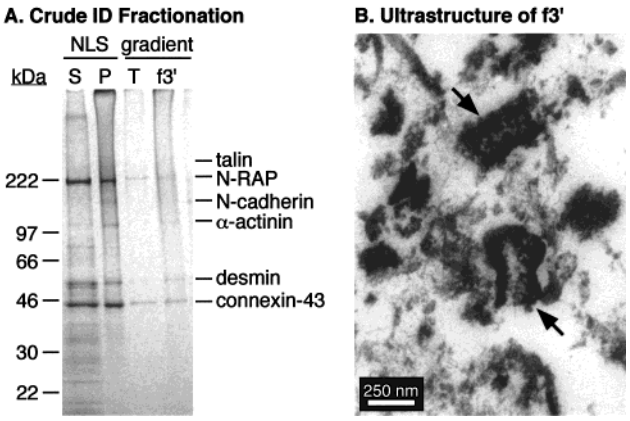

FIGURE 8: (A) Gel electrophoresis of the fractions collected after detergent extraction of the crude intercalated disk fraction (F3) with *N*-lauryl sarcosinate (NLS), followed by sucrose gradient centrifugation of the insoluble pellet. Labeling and loading is as described for Figure 7. Proteins identified as present in the F3′ fraction by immunoblot are labeled. No β1-integrin, vinculin, myosin heavy chain, or actin was detected in this fraction. (B) Transmission electron microscopy of the F3′ fraction reveals the presence of extracted fragments of intercalated disks (arrows).

constituents identified by immunoblot are visible in the Coomassie-stained gel (Figure 8A). Densitometry of the Coomassie-stained gels shows that approximately 0.5% of the total homogenate protein was recovered in the final F3′ fraction. We estimate that N-RAP and connexin 43 are enriched 100−200-fold in this fraction, while N-cadherin and desmin are enriched 50−100 fold, talin is enriched 10−20-fold, and α-actinin is enriched 5−10-fold. Furthermore, transmission electron microscopy of the F3′ fraction reveals the presence of extracted fragments of intercalated disks (Figure 8B, arrows).

N-RAP Binding to α-Actinin. Although N-RAP is not known to bind any of the proteins found in the F3′ fraction except talin, we recently observed that N-RAP−IB, the region of N-RAP between the N-RAP LIM domain and the N-RAP superrepeats, colocalizes with α-actinin at Z-lines when expressed as a GFP fusion protein in cultured embryonic chick cardiomyocytes (*25*). Therefore, we used a gel overlay assay to test for direct binding between α-actinin and recombinant N-RAP fragments. Figure 9A illustrates the regions of N-RAP that we expressed as histidine-tagged fusion proteins. Following electrophoresis of the purified proteins (Figure 9B) and transfer to PVDF membrane, these proteins were incubated with purified α-actinin. After extensive washing, bound α-actinin was detected by an anti-α-actinin antibody. Using this assay, we detected significant α-actinin binding to N-RAP−IB and N-RAP−LIM (Figure 9C). In contrast, α-actinin did not bind N-RAP−SR or either of the histidine-tagged CAT proteins (HIS−CAT-1 and HIS−CAT-2) (Figure 9C). Simultaneously run control membranes that were not incubated with α-actinin demonstrated specific detection of electrophoresed α-actinin but no detection of any of the target proteins (data not shown).

DISCUSSION

Previously, we demonstrated by northern blots that the N-RAP message is found in skeletal muscles and heart but is not found in a variety of nonmuscle tissues (*1*). The present

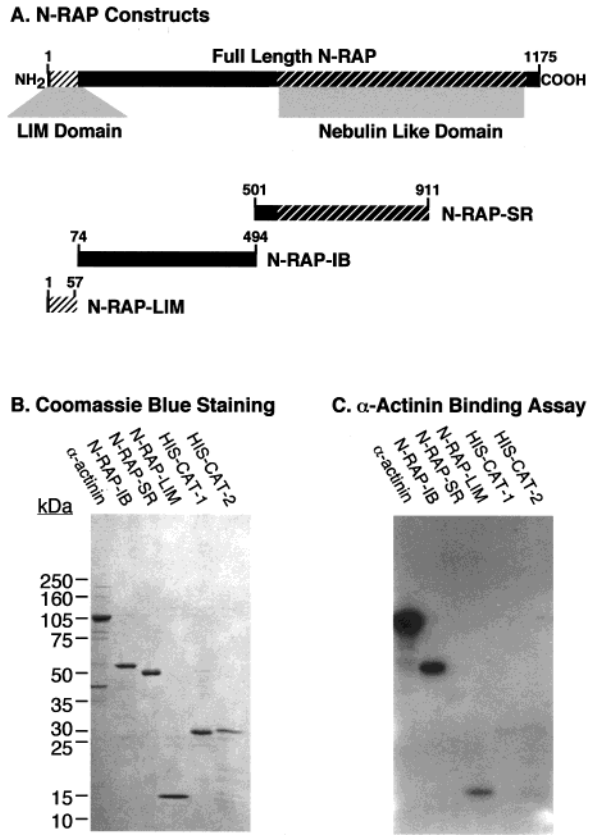

FIGURE 9: (A) Schematic diagram showing the domain organization of N-RAP (top), along with the regions of N-RAP expressed as histidine-tagged fusion proteins. Numbers refer to amino acid residues from the full-length mouse N-RAP sequence. (B, C) α-Actinin binding to blotted proteins. Duplicate loadings were used for total protein detection with Coomassie blue (panel B) and for detection of α-actinin binding (panel C). Lanes were loaded with purified proteins as indicated. The histidine-tagged CAT proteins (HIS−CAT-1 and HIS−CAT-2) served as negative controls. Significant α-actinin binding was observed for recombinant N-RAP−IB and N-RAP−LIM.

results expand these findings to show that the N-RAP protein is only expressed in the striated muscles but is not detected in a variety of nonmuscle tissues; furthermore, N-RAP was not detected in tissues rich in smooth muscle cells, such as the stomach and uterus (Figure 1). The results clearly demonstrate that N-RAP is only found in the tissues that produce striated myofibrils.

The previous identification of N-RAP at skeletal muscle myotendon junctions and cardiac intercalated disks suggested an association of N-RAP with the ends of myofibrils (*1*). Ultrastructural observations in both skeletal muscles (*8*) and the heart (Figure 2) support this; in both cases, immunoelectron microscopy showed that N-RAP is concentrated at the terminal actin filaments that link the myofibrils to the cell membranes. Interestingly, vinculin antibodies generally labeled close to the fascia adherens membrane, while the N-RAP antibody was detected close to the membrane as well as inside the terminal cell processes. A similar relative distribution of vinculin and α-actinin in cardiac muscle was demonstrated by Tokuyasu et al. (*16*). α-Actinin may function in actin−membrane association (*26*) as well as actin filament cross-linking (*27*) and may play both roles at cardiac adherens junctions. Thus, the distribution of N-RAP suggests that it may bind to vinculin in vivo but that it may also play a role in organizing the terminal cytoskeletal filaments at intercalated disks.

Previous investigators have attempted biochemical purification of defined regions of the cardiac intercalated disks (*21*, *28*, *29*). In general, these early studies were performed before the widespread use of immunoblotting techniques became common. By revisiting the biochemical isolation of these structures and probing the fractions with widely available antibody reagents, we could monitor the copurification of N-RAP with the key constituents of intercalated disks. We successfully isolated a fraction, F3, that was enriched for N-cadherin, connexin 43, and β1-integrin and that contained virtually all of the cellular N-RAP. Morphologically, this fraction was enriched for fragments of intercalated disks, and the fasciae adherentes fragments stained positively for both N-RAP and vinculin. Detergent extraction followed by sucrose gradient centrifugation succeeded in removing residual actin and myosin from this fraction, as well as vinculin and the β1-integrins. The resulting fraction still contained most of the cellular N-RAP, along with talin, N-cadherin, α-actinin, desmin, and connexin 43, and ultrastructural examination revealed many fragmented pieces of intercalated disks. These data show that N-RAP remains associated with intercalated disk constituents, even after the complete removal of actin. N-RAP also remains bound at the ends of isolated myofibrils, even after extraction with detergent (Figure 3). The biochemical evidence supports the hypothesis that N-RAP is part of the mechanical link between the myofibrils and the intercalated disks.

The available evidence does not exclude the possibility that N-RAP has a regulatory function. Previous studies have demonstrated that several cytoskeleton-associated LIM domain proteins are phosphorylated (*30*−*32*). In the case of paxillin, LIM domain phosphorylation regulates paxillin accumulation at focal contacts as well as cell adhesion to fibronectin (*30*). In addition to its proposed mechanical role in adult striated muscles, N-RAP has recently been implicated in myofibril assembly (*9*, *25*). Whether N-RAP plays a regulatory role in the assembly of myofibrils or junctional complexes such as intercalated disks remains to be investigated.

The details of the membrane to myofibril linkage remain to be determined. Binding studies, however, suggest several models. Our previous work on N-RAP led to the hypothesis that N-RAP is a component of an integrin-mediated membrane−myofibril link (*7*). In this scheme, the terminal actin filaments of the myofibrils bind the repetitive actin binding domains present in the N-RAP superrepeats, while the N-RAP LIM domain binds talin, which in turn is bound to the membrane-spanning β1-integrin. This simple scheme can be made more complex by considering talin (*33*−*35*) and vinculin (*36*−*38*) binding to the actin filaments, as well as to each other (*39*−*41*), along with vinculin binding to N-RAP (*7*). All of these components are concentrated at the myotendinous junctions of skeletal muscles (*42*−*44*), where the β1D-integrin isoform is thought to attach this chain of proteins to the extracellular matrix (*18*). However, N-RAP is the only muscle-specific constituent in this group of linking proteins.

At the cardiac intercalated disk, the molecular constituents of the integrin system remain to be definitively determined.

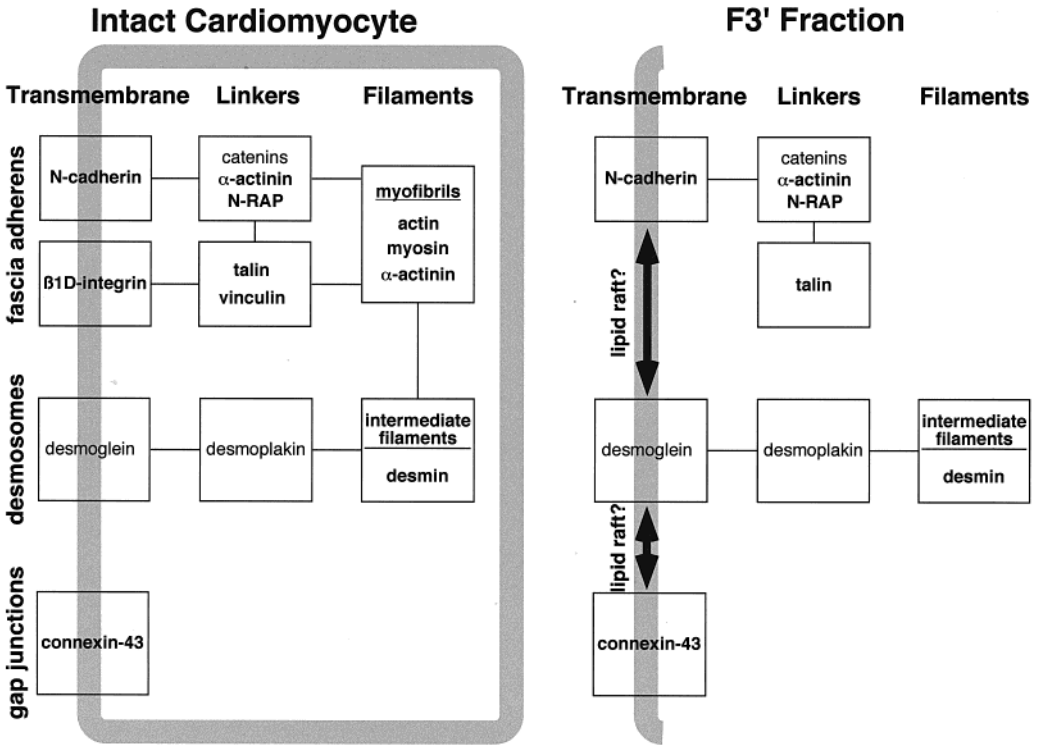

FIGURE 10: Schematic diagram of the regions of the cardiac intercalated disk, the major transmembrane proteins present in each region, and intracellular linking and filamentous proteins to which they connect. The left-hand side depicts interactions in the intact cardiomyocyte, including putative integrin and cadherin-mediated membrane−myofibril links, while the right-hand side illustrates interactions in the highly purified F3′ fraction, which is devoid of myofibrils and integrins. Proteins analyzed during intercalated disk purification are shown in boldface type. See text for details.

Using similar techniques, one group was able to detect talin at the intercalated disk (*17*), while two other groups concluded that talin is not present at these junctions (*45*, *46*). In addition, the question of whether there are extracellular matrix proteins to which the integrins might attach in the space between the cells at the intercalated disk remains unresolved. In cardiac muscle, the situation is further complicated by the presence of cadherin-mediated links between adjoining cells at the intercalated disks (*12*−*15*). In many tissue types, the cadherin system is known to link the actin cytoskeleton to the membrane by binding to the catenins, which in turn bind the actin cross-linker α-actinin (*14*, *47*, *48*).

Although both N-cadherin and β1D-integrin are present at the cardiac intercalated disk, it is not known if one or both of these systems is responsible for mechanically linking the myofibrils to the cytoplasmic face of the adherens junction. Figure 10 illustrates putative integrin and cadherin-mediated membrane−myofibril links, along with the major proteins that may be involved. Linkages that may be present in the intact cardiomyocyte are illustrated (Figure 10, left panel) along with those that may persist in the highly purified F3′ fraction (Figure 10, right panel). The finding that N-RAP copurifies with detergent-extracted intercalated disk fragments even though β-integrin and vinculin have been completely removed suggests that N-RAP association with the adherens junction region is mediated by the cadherin system (Figure 10). Our finding that recombinant N-RAP fragments bind α-actinin in a gel overlay assay is consistent with this hypothesis. In addition, since it binds N-RAP in vitro, the talin found in the F3′ fraction may be bound to N-RAP (Figure 10), suggesting a role for N-RAP in cross-linking components of the cadherin and the integrin systems at the adherens junction.

Finally, the copurification of N-cadherin, connexin 43, and desmin in the F3′ fraction suggests that the physical association of the adherens junctions, gap junctions, and desmosomes within the intercalated disk is maintained even after detergent extraction with *N*-lauryl sarcosinate. The biological importance of detergent-resistant membrane domains, or lipid rafts, has recently been recognized (*49*). The epithelial tight junction is one example of an intercellular junction with raftlike properties (*50*); our results suggest that the cardiac intercalated disk may also belong to this class of membranes (Figure 10, right panel).

ACKNOWLEDGMENT

We thank Amy H. Herrera for excellent technical assistance.

REFERENCES

1. Luo, G., Zhang, J. Q., Nguyen, T. P., Herrera, A. H., Paterson, B., and Horowits, R. (1997) *Cell Motil. Cytoskeleton 38*, 75−90.
2. Wang, K., and Wright, J. (1988) *J. Cell Biol. 107*, 2199−2212.
3. Labeit, S., Gibson, T., Lakey, A., Leonard, K., Zeviani, M., Knight, P., Wardale, J., and Trinick, J. (1991) *FEBS Lett. 282*, 313−6.
4. Kruger, M., Wright, J., and Wang, K. (1991) *J. Cell Biol. 115*, 97−107.
5. Sanchez, G. I., and Rabbitts, T. H. (1994) *Trends Genet. 10*, 315−20.
6. Dawid, I. B., Breen, J. J., and Toyama, R. (1998) *Trends Genet. 14*, 156−62.

7. Luo, G., Herrera, A. H., and Horowits, R. (1999) *Biochemistry 38*, 6135−43.
8. Herrera, A. H., Elzey, B., Law, D. J., and Horowits, R. (2000) *Cell Motil. Cytoskeleton 45*, 211−222.
9. Carroll, S. L., and Horowits, R. (2000) *Cell Motil. Cytoskeleton 47*, 63−76.
10. Forbes, M. S., and Sperelakis, N. (1985) *Tissue Cell 17*, 605−48.
11. Severs, N. J. (1995) *Histol. Histopathol. 10*, 481−501.
12. Takeichi, M. (1990) *Annu. Rev. Biochem. 59*, 237−52.
13. Geiger, B., and Ayalon, O. (1992) *Annu. Rev. Cell Biol. 8*, 307−32.
14. Kemler, R. (1993) *Trends Genet. 9*, 317−21.
15. Hertig, C. M., Eppenberger-Eberhardt, M., Koch, S., and Eppenberger, H. M. (1996) *J. Cell Sci. 109*, 1−10.
16. Tokuyasu, K. T., Dutton, A. H., Geiger, B., and Singer, S. J. (1981) *Proc. Natl. Acad. Sci. U.S.A. 78*, 7619−23.
17. Belkin, A. M., Zhidkova, N. I., and Koteliansky, V. E. (1986) *FEBS Lett. 200*, 32−6.
18. Belkin, A. M., Zhidkova, N. I., Balzac, F., Altruda, F., Tomatis, D., Maier, A., Tarone, G., Koteliansky, V. E., and Burridge, K. (1996) *J. Cell Biol. 132*, 211−26.
19. Hertig, C. M., Butz, S., Koch, S., Eppenberger-Eberhardt, M., Kemler, R., and Eppenberger, H. M. (1996) *J. Cell Sci. 109*, 11−20.
20. Wang, S. M., and Greaser, M. L. (1985) *J. Muscle Res. Cell Motil. 6*, 293−312.
21. Colaco, C. A., and Evans, W. H. (1981) *J. Cell Sci. 52*, 313−25.
22. Towbin, H., Staehelin, T., and Gordon, J. (1979) *Proc. Natl. Acad. Sci. U.S.A. 76*, 4350−4.
23. Tokuyasu, K. T. (1989) *Histochem. J. 21*, 163−71.
24. Law, D. J. (1993) *J. Muscle Res. Cell Motil. 14*, 401−11.
25. Carroll, S. L., Herrera, A. H., and Horowits, R. (2000) *Mol. Biol. Cell 11*, 77a.
26. Otey, C. A., Pavalko, F. M., and Burridge, K. (1990) *J. Cell Biol. 111*, 721−9.
27. Wachsstock, D. H., Schwartz, W. H., and Pollard, T. D. (1993) *Biophys. J. 65*, 205−14.
28. Colaco, C. A., and Evans, W. H. (1982) *Biochim. Biophys. Acta 684*, 40−6.
29. Kensler, R. W., and Goodenough, D. A. (1980) *J. Cell Biol. 86*, 755−64.
30. Brown, M. C., Perrotta, J. A., and Turner, C. E. (1998) *Mol. Biol. Cell 9*, 1803−16.
31. Schreiber, V., Moog-Lutz, C., Regnier, C. H., Chenard, M. P., Boeuf, H., Vonesch, J. L., Tomasetto, C., and Rio, M. C. (1998) *Mol. Med. 4*, 675−87.
32. Zhou, Q., Ruiz-Lozano, P., Martone, M. E., and Chen, J. (1999) *J. Biol. Chem. 274*, 19807−13.
33. Hemmings, L., Rees, D. J., Ohanian, V., Bolton, S. J., Gilmore, A. P., Patel, B., Priddle, H., Trevithick, J. E., Hynes, R. O., and Critchley, D. R. (1996) *J. Cell Sci. 109*, 2715−26.
34. Muguruma, M., Matsumura, S., and Fukazawa, T. (1990) *Biochem. Biophys. Res. Commun. 171*, 1217−23.
35. Zhang, J., Robson, R. M., Schmidt, J. M., and Stromer, M. H. (1996) *Biochem. Biophys. Res. Commun. 218*, 530−7.
36. Johnson, R. P., and Craig, S. W. (1995) *Nature 373*, 261−4.
37. Huttelmaier, S., Bubeck, P., Rudiger, M., and Jockusch, B. M. (1997) *Eur. J. Biochem. 247*, 1136−42.
38. Menkel, A. R., Kroemker, M., Bubeck, P., Ronsiek, M., Nikolai, G., and Jockusch, B. M. (1994) *J. Cell Biol. 126*, 1231−40.
39. Price, G. J., Jones, P., Davison, M. D., Patel, B., Bendori, R., Geiger, B., and Critchley, D. R. (1989) *Biochem. J. 259*, 453−61.
40. Johnson, R. P., and Craig, S. W. (1994) *J. Biol. Chem. 269*, 12611−9.
41. Gilmore, A. P., and Burridge, K. (1996) *Nature 381*, 531−5.
42. Tidball, J. G., O'Halloran, T., and Burridge, K. (1986) *J. Cell Biol. 103*, 1465−72.
43. Tidball, J. G. (1991) *J. Biomech. 24* (*Suppl. 1*), 43−52.
44. Shear, C. R., and Bloch, R. J. (1985) *J. Cell Biol. 101*, 240−56.
45. Drenckhahn, D., Beckerle, M., Burridge, K., and Otto, J. (1988) *Eur. J. Cell Biol. 46*, 513−22.
46. Geiger, B., Volk, T., and Volberg, T. (1985) *J. Cell Biol. 101*, 1523−31.
47. Nieset, J. E., Redfield, A. R., Jin, F., Knudsen, K. A., Johnson, K. R., and Wheelock, M. J. (1997) *J. Cell Sci. 110*, 1013−22.
48. Knudsen, K. A., Soler, A. P., Johnson, K. R., and Wheelock, M. J. (1995) *J. Cell Biol. 130*, 67−77.
49. Brown, D. A., and London, E. (1998) *Annu. Rev. Cell Dev. Biol. 14*, 111−36.
50. Nusrat, A., Parkos, C. A., Verkade, P., Foley, C. S., Liang, T. W., Innis-Whitehouse, W., Eastburn, K. K., and Madara, J. L. (2000) *J. Cell Sci. 113*, 1771−81.

BI0107445